A metaheuristic segmentation framework for detection of retinal disorders from fundus images using a hybrid ant colony optimization

D. Devarajan, S. M. Ramesh & B. Gomathy

Soft Computing
A Fusion of Foundations, Methodologies and Applications

ISSN 1432-7643
Volume 24
Number 17

Soft Comput (2020) 24:13347-13356
DOI 10.1007/s00500-020-04753-7

Springer

Soft Computing (2020) 24:13347–13356
https://doi.org/10.1007/s00500-020-04753-7

METHODOLOGIES AND APPLICATION

A metaheuristic segmentation framework for detection of retinal disorders from fundus images using a hybrid ant colony optimization

D. Devarajan[1] · S. M. Ramesh[1] · B. Gomathy[2]

Published online: 12 February 2020

Abstract
Imaging modalities play a major role in early detection and diagnosis of various medical conditions related to the patient. Retinal image segmentation has been taken up for investigation in this research paper to efficiently detect the presence of eye disorder which could be indicators of major onset of conditions like hypertension, cataracts, diabetic retinopathy, age-related macular disorders, etc. A machine learning method for classification of given pixels in the search space into regions containing blood vessels and those that do not contain blood vessels is implemented using a three-stage neural classifier in this paper. Prior to classification, an optimization algorithm namely ant colony optimization derived from nature-inspired phenomena is used to provide an optimal feature vector set to set high standards for the neural network based classification approach. The novelty and merits of the paper lie in back tracing of the segmentation process in which optimization is done first on the preprocessed features followed by classification for segmented output on the optimized features. This results in elimination of redundant feature vectors which tend to occupy much memory as well increase the computational overhead on the process. The entire implemented system is automated by the machine learning process and tested on 30 samples, 15 each on DRIVE and STARE databases. Classification rates of nearly 98% on an average scenario have been achieved for segmentation and 96.5% for abnormality detection. The performances have been compared against Bayesian set models and standalone ANN models.

Keywords Retinal image segmentation · Fundus images · DRIVE · STARE · Ant colony optimization · Neural network classifier · Classification accuracy

1 Introduction

Clinical imaging has witnessed a great revolution in recent times especially with the advent of state-of-the-art imaging systems and modalities. Clinical imaging has attracted a wide range of research interests due to their immense potential in early detection of medical conditions. This early detection helps in appropriate treatment through diagnosis thereby resulting in near elimination of the medical condition. An interesting feature to be observed in clinical imaging is that multiple symptoms and conditions could be decided upon from the same imaging modality. For example, retinal imaging could help in detection of cataract, blurriness of eyes, etc. Additionally, it also plays to be a vital indicator of certain blood-related conditions such as diabetes and hypertension. Hence, the role of medical imaging has been dominant in almost all health-care sectors resulting in drastic reduction in the mortality rate due to late detections. The issue of retinal imaging for detection of disorders related to retina of the eye has been taken as the primary issue of investigation in this research paper. The process of retinal image processing for detection of early disorders is quite a challenging task with several constraints related to extraction of the retina from the background. It could be inferred on the whole that the

Communicated by V. Loia.

✉ D. Devarajan
devarajan@egspec.org

S. M. Ramesh
drsmramesh@egspec.org

B. Gomathy
gomramesh@gmail.com

[1] E.G.S Pillay College of Engineering and Technology, Nagapattinam, Tamilnadu, India

[2] Bannari Amman Institute of Technology, Erode, Tamilnadu, India

overall efficiency of the detection as well as classification process relies to a great extent on the quality of background extraction method applied on the fundus images. A typical retinal fundus image is shown in Fig. 1.

Figure 1 clearly illustrates a high-resolution image of the retina taken from the DRIVE database (digital retinal images for vessel extraction) with an optic disk and a network of optic nerves. It could be observed that the complex network of optic nerves is a pure indicator of any retinal disorder condition. A number of retinal disorders could be inferred from the literature (Wong et al. 2002) which include retinal tear which may occur due to a sudden flashing light which causes considerable damage to the gel-like substance in the middle of the retina. Filling up of fluid under the retina leads to retinal lifting from tissue or retinal detachment, while blurred vision may result due to pulling of retina by the epiretinal membrane. Injury to the eye may result in a hole in the center of retina resulting in a condition known as macular hole, while retinal degeneration and severe blurring may result due to macular degradation. Blood vessels in the retina are clear indicators of diabetic retinopathy as they begin to swell in affected patients and cause leakage of fluid into and under the area below the retina. Another disorder related to blurred vision in retinitis pigmentosa which is a kind of degenerative disease. A statistical analysis by World Health Organization (WHO) (Nazimul et al. 2008) has been presented indicating the analysis of percentage of blind people due to several syndromes and disorders which include trachoma, glaucoma, age-related macular disorders (AMD) and cataract.

As shown in Fig. 2, it could be seen that a five-period/sample analysis indicates that cataract and glaucoma are found to be major contributors to the overall blindness ratio

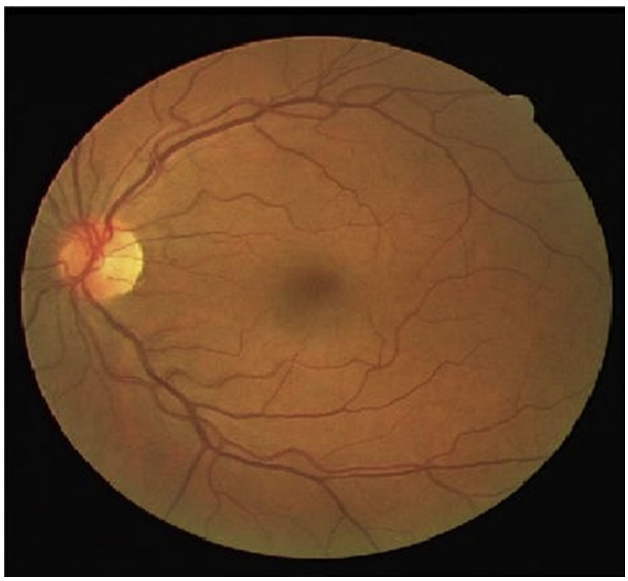

Fig. 1 Retinal fundus image (DRIVE database)

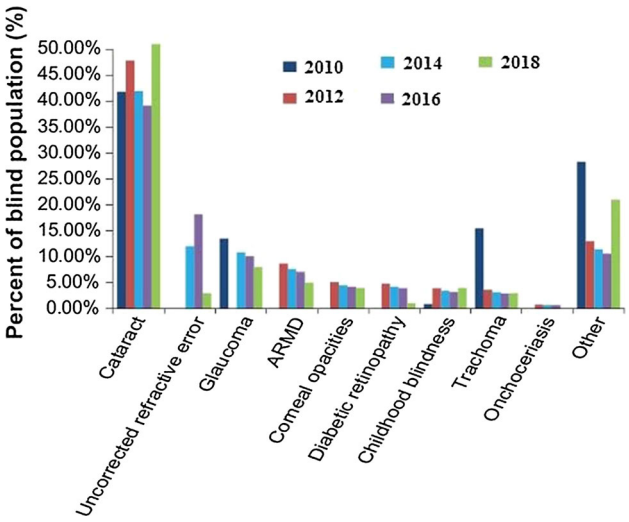

Fig. 2 WHO statistics of percentage of eye-related disorders on a global scale (WHO 2018)

if left undetected or not detected at an early stage. The other factors result from intentional and unintentional eye injuries due to exposure to chemicals, accidents, etc. Hence, this analysis has proved to be a motivating factor behind this research work as it clearly indicates the role of retinal imagining for early detection and diagnosis of medical conditions. It has also been predicted by WHO that by 2020, the percentage of AMD and diabetic retinopathy is projected to rise by up to 47% by 2024 and an alarming 71% by 2034 if left unchecked. Cataract is also found to be rising at an alarming rate making to be one of the major contributors to apparent blindness in age groups exceeding 64 years and those with diabetic history. In real time, optical coherence tomography (OCT) technology helps pathologists and medical experts to view cross-sectional views of retina in real time for detection of some kinds of macular disorders. However, the precision of detection using OCT is sometimes limited by media opacity (Lee et al. 2010; Savastano et al. 2014) and the presence of cataract interference on the imaging system. Improvement of this method is the ultra-wide field scanning ophthalmoscope (SLO) (Inoue et al. 2013) which helps in a wider viewing area of the retina thus improving the resolution. However, cataract presence still contributes to limiting the performance of these real-time methods. Hence, conventional methods of foreground and background removal extract the blood vessels which are clear indicators of the medical condition is followed and experimented in this research paper. A metaheuristic method is experimented in this research paper with concepts of optimization using evolutionary algorithms to improve the detection accuracy within the shortest period of time possible. The paper is organized into a brief overview of survey related to various segmentation methods in Sect. 2. The next section presents

the proposed evolutionary framework for efficient detection of retinal disorders followed by analysis of the experimental results in Sect. 4. Section 5 summarizes the findings of the paper with a note on the future scope of this work.

2 Related work

Research in imaging and various imaging modalities toward medical health care and early detection of medical conditions has been gaining widespread significance aided by various state-of-the-art imaging techniques and algorithms put forward by researchers to improve the accuracy and precision. In lines with the objective of this paper, retinal image processing has witnessed quite a great deal of revolution due to its inherent capability to provide vital information regarding onset of various disorders related to old age and diabetes (Elbalaoui et al. 2017). Kumar and Shimna (2017), age-related macular disorders and diabetic retinopathy are quite some of the essential disorders that could be detected with accurate and systematic retinal image processing. Retinal image processing consists of three essential steps, namely preprocessing followed by morphological or frequency domain processing for extraction of features followed by classification of the condition. Several techniques have been proposed in the literature related to preprocessing (Ponraj et al. 2011) which include simple filtering techniques which define a mask of $N \times N$ dimensions depending on the patch size to remove noise which accompany with the imaging modality. Common noise forms include the Gaussian and speckle noise (Samuel Manoharan 2019). The second stage of processing which include morphological processing includes foreground extraction/background removal to extract the blood vessels or the exudates which are present on the retinal surface. Fusion-based methods (Kathiresan and Samuel Manoharan 2013) have been actively investigated in the literature to utilize two perspectives or modalities of the same image and fuse together the information for removal of the region of interest (ROI).

A significant contribution has been observed in the literature toward morphological processing for detection through extraction of blood vessels from the retinal blood vessels. These include the well-known histogram equalization methods. This method is based on classifying pixels based on the presence or absence of blood vessels in the pixel. However, increased time consumption and average precision is observed in this method. The speed of the segmentation process is considerably increased by utilizing Gaussian pyramid-based structures which form a hierarchical form of decomposition of the fundus image. Level zero represents the original images and further levels obtained by halving of the previous-level images. Neighborhood analysis methods are used for classifying vessels into the presence/absence of blood vessels. This pyramidal decomposition is implemented using a filter bank structure in the frequency domain using the curvelet transform (Miri and Mahloojifar 2011) which is best suited for approximating images with smooth contours which is the characteristic of the retinal fundus images. However, the method lacks precision as the blood veins and arteries do not at all times follow a smooth contour resulting in error generation.

However, observation from the literature indicates that the manual method of segmentation using log transforms, top hat transforms and erosion/dilations tend to increase the segmentation time with an average accuracy rate especially when data set size and resolutions are considerably higher, which have been undergoing a rapid transition toward automated methods (Ponraj et al. 2011). Supervised methods involving neural networks (Marin et al. 2011) for classification based on features extracted from the retinal image have been found to improve the precision of detection by bringing down the false negatives. This has been made possible by utilizing two feature set-based methods involving moment invariant features as well as gray level differences. SVM-based methods have also been used as a powerful classifier alternate (Vijayakumari and Suriyanarayanan 2012). This has been made possible to a great extent with the advent of machine learning and soft computing methods which tend to automate the entire process through series/sequences of learning and training imparted to the networks. Neural networks have played a major role in automation process by imparting knowledge and intelligence to the segmentation algorithm to automatically detect, segment and classify the disorder through intensive training imparted to the neural nodes and layers which form the platform of the same.

As mentioned in the previous sections, exudates are important indicators which denote onset of retinal tear, rapidly progressing diabetic retinopathy or leakage of fluid into retina and segmentation of exudates have been given special interest in the literature. Intelligence has been inducted into the segmentation system through fuzzy-based modules (Osareh et al. 2009) consisting of a c-means clustering for neighborhood detection. Hybrid methods have been put forward through genetic-based optimization for ranking the features extracted through the c-means clustering process. A 92.5% sensitivity levels have been reported in this method for a database containing 300 retinal fundus images. Other optimization methods implemented in the literature include ant colony optimization (Rahebi and Hardalac 2016) for extraction and classification of feature vectors but are found to lack precision as well as increasing computational overhead (Pereira et al. 2015) due to the combined function of extraction followed

by segmentation done by a single optimization method. This causes a trade-off imbalance resulting in improvement at the cost of another. Other optimization algorithms investigated in the literature (Mareli and Twala 2018) include bacterial foraging, cuckoo search and firefly algorithms (Das et al. 2009). Automation in detection (Lupascu et al. 2010) has also been investigated through a two-stage morphological processing filters, namely vesselness filter (Szénási 2014) and adaptive threshold filter to extract the vessels from the background. Complex wavelet-based methods (You et al. 2011) have been effectively used to establish a proper balance between extraction of thin and thick blood vessels by using concepts of radial projection and semi-supervised learning approach. Similar implementations involving scale-level processing have been observed in the literature (Li et al. 2012) where issue of noise corruption of tiny blood vessels has been resolved using methods of width estimation of these small vessels. This has been achieved by multiplying the matched filter responses at each associated scales. This width-based segmentation method is found to improve the quality of the tiny blood vessels in the retinal image.

Automated methods of segmentation not only include blood vessels but also the optic disk which is used to relate to a number of disorders. The process is quite inverse (Elbalaoui et al. 2018; Hoover et al. 2000) where the optic disk is segmented out leaving behind the blood vessels and the macular regions in the background.

3 Problem formulation

Retinal image processing is an essential aspect related to medical image processing and has been fruitful in early detection and diagnosis of cataracts, diabetic retinopathy and hypertension. Efficient methods of segmenting the retinal blood vessels or optic disk define the degree of overall accuracy. Considering the retinal fundus image $r(x, y)$ and the response of the channel characterized by additive white Gaussian noise as well as multiplicative speckle noise with cumulative variance , the objective of the proposed research work is to obtain a binary hypothesis related to classification of blood vessel to normal or abnormal, and hence formulated as

$$r_c(x,y) = \begin{vmatrix} 1, & abnormal\ blood\ vessel \\ 0, & normal\ blood\ vessel \end{vmatrix} \quad (1)$$

In Eq. (1), $r_c(x, y)$ denotes the classified output, and '1' represents the presence of abnormality in the segmented output, while a 0 indicates normalcy in the segmented blood vessel. However, the classification depends on the feature vector set which is optimized by using ACO in the proposed work and formulated as

$$S_k(x,y) = O_{min}(F(\bar{x},y) \in R_n; n = 1,2,3\ldots255 \quad (2)$$

Based on the problem formulated as per (1) and (2), a evolutionary algorithm-based neural classifier has been proposed in the next section.

4 Proposed work

The proposed algorithm focuses toward providing an optimal and efficient classification of retinal blood vessels for early detection of diabetic retinopathy as well as AMD. The proposed problem follows a backtracking propagation where the classification using neural network model is based on a set of optimal feature vectors which are trained using the extracted features using an optimization algorithm, namely ant colony which best mimics the real-time scenario. Hence, the proposed algorithm is labeled as hybrid optimized neural classifier (HONC) which combines the merits of optimized feature set using ACO coupled together with the classifying features of neural networks. This section presents a brief modeling of the ACO as well as the neural network models followed by the pseudocode of the proposed algorithm.

4.1 Ant colony algorithm

Ant colony algorithm is one of the well-known and powerful optimization algorithms which derive its behavior from the naturally evolving phenomena in real time. This algorithm is analogous to the food foraging behavior of ants and is used to select the best possible solution in a given search space. A typical illustration of the ant colony optimization methodology is shown in Fig. 3.

The algorithm is similar to any other food foraging algorithms/phenomena as observed in the well-known bee algorithm, particle swarm algorithm, etc., where the ants go in search of food source. An interesting feature to be observed is that the ants leave behind a trail of a specific hormone known as pheromone as they go in search of the food source. Based on the availability of quantity of food source and the shortest optimal path which they undertake, the level of pheromone secretion is taken as the measure to

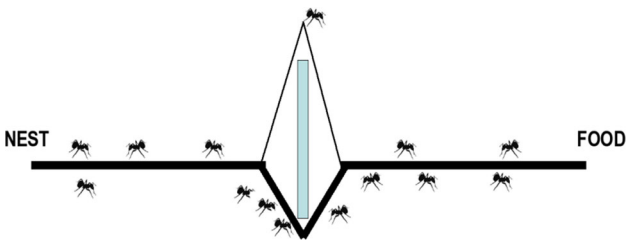

Fig. 3 Ant colony foraging illustration

determine the path toward optimal solution. Pheromone has a tendency to evaporate, and hence the quantity of pheromone where the ants are less frequent is minimal when compared to the path that is most frequent. This indicates the direction of the best solution resulting in drastic reduction in search space thus accounting for the reduced convergence time. As seen from the above figure, the process of food foraging is initiated by a set of ants who scout the area or the surroundings for the presence of food particles in a random fashion. As the process is initiated in search of the food source, the position of any ant at a point of time t is updated from $\vec{p}_1$ *to* $\vec{p}_2$ in the search space defined in the interval $[-1, +1]$. The position update equation is accordingly formulated as

$$\overrightarrow{\boldsymbol{p}_{\boldsymbol{new},t}} = \vec{\boldsymbol{p}}_{0,t} + \boldsymbol{Real} * \boldsymbol{Randint}[-1, 1] \tag{3}$$

At each iteration, the optimality of the current location $\vec{p}_{new,t}$ is tested based on the amount of pheromone trail left behind the current direction. On obtaining a new update in the $+1$ direction, the location of the ant is further updated as follows.

$$\overrightarrow{\boldsymbol{p}_{\boldsymbol{new},t}}(\boldsymbol{n}+1) = \vec{\boldsymbol{p}}_{\boldsymbol{previous},t}(\boldsymbol{n}) + \left(\overrightarrow{\boldsymbol{l}_{j,t}}(\boldsymbol{n}) - \vec{\boldsymbol{l}}_{i,t}(\boldsymbol{n})\right) * \boldsymbol{Randint}[0, 1] \tag{4}$$

The process as in (4) is repeated until the point of convergence is reached. The process terminates itself when no more food source is available or no more shortest/optimal paths are available in the specified trail path. At each point of time, the inter-distance between the ants based on their position update is computed using the well-known Euclidean distance parameter and updated into (4) for finding the next possible step of the ant. The concept of ACO is depicted as a flow process shown in Fig. 4.

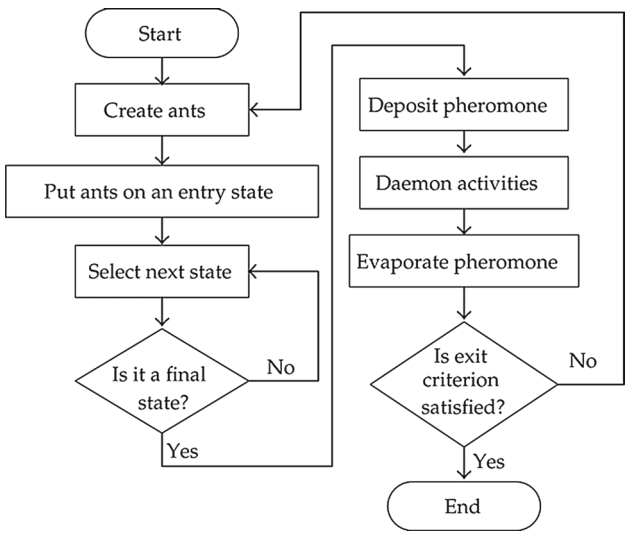

Fig. 4 Flow process of ACO

Analogously, this is applied to the proposed work of retinal image segmentation to extract optimal and necessary set of features required for the segmentation to be complete and precise. Given a search space which resembles the set of all features in the retinal image, the objective of the ACO in the given case is to find the best possible set of feature vectors as specified in (2) which are optimized with respect to distance as well as their dimensions. Reduction in dimension is accounted for by eliminating redundant pixels or repeating positions of ants. Based on K iterations of the ACO carried out in the image search space $r(x, y) \in R$, the set of optimal feature vectors are given as

$$\vec{F}(x, y) = \min[r(x, y] = \emptyset\left(z_1, z_2, z_3, \ldots z_n\right) \tag{5}$$

4.2 Neural network model

The proposed neural network model in the latter half of this system plays a vital role by learning the feature vectors generated from (5) in the previous section and provides a decision-based classification output. A three-layer feedforward neural network model is utilized in the proposed work as shown in Fig. 5.

Based on the above formulations, the proposed work could be modeled as shown in Fig. 6.

The proposed flow as shown in Fig. 6 could be classified into three modules, namely signal preprocessing, feature extraction and segmentation and classification using hybrid HONC algorithm.

4.3 Signal acquisition and Preprocessing

The input retinal image is obtained and subjected to preprocessing using a mean–median hybrid filter to remove the peaks followed by histogram equalization for uniform distribution of intensity values. Smoothening is provided by the mean filter.

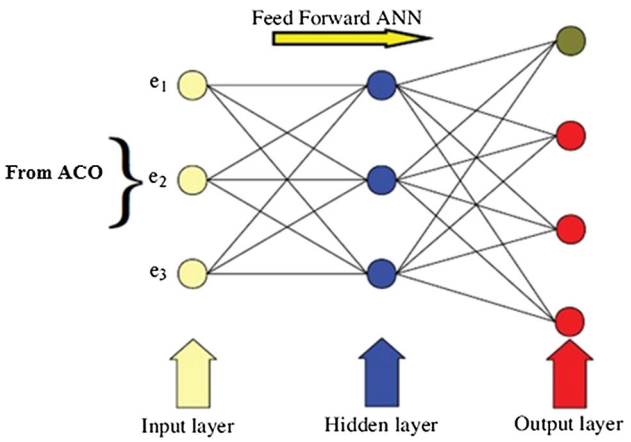

Fig. 5 Feedforward ANN architecture in proposed NNACOR

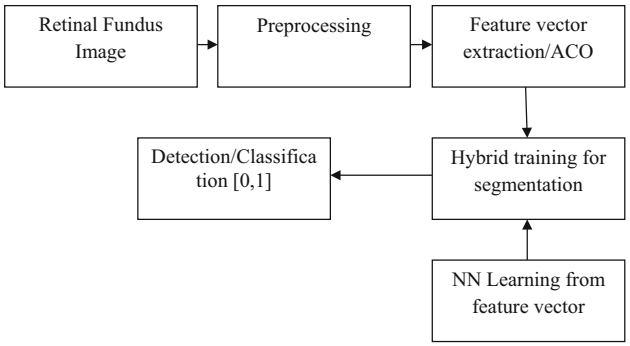

Fig. 6 Flow process of proposed HONC for retinal image segmentation

4.4 Proposed HONC model

Following the preprocessing stage, the image is subjected to the hybrid module consisting of the ACO for feature extraction followed by learning and training to classify the type of output into normal and abnormal output. The pseudocode for the proposed algorithm is presented as two sections, namely ACO for feature selection followed by neural classifier for providing the output of segmentation.

The pseudocode of the ACO for feature extraction is given below.

$Input: Preprocessed\ image\ R_p(x,y) \in R$
$Output: Feature\ vector\ \vec{F} \in R$
$initialize\ n: population\ of\ ants$
$assert\ \emptyset = set\ of\ all\ features \in R$
$begin$
  $for\ i = 0\ to\ \emptyset_{opt};$
    $for\ j = 0\ to\ N_{\emptyset_t}(current\ feature\ count)$
      $\emptyset_{total} = \sum(\emptyset_{selected} + \emptyset(N_{\emptyset_t})$
    $call\ ACO(\emptyset_{total})$
      $update\ p_{new} = p_{old} + \Delta$
    $update\ best\ ant = min\|\emptyset\|\epsilon[R]$
end

The pseudocode of the proposed hybrid ACO-based neural classifier (HCON) algorithm is given below.

$Input: Feature\ vectors\ \vec{F} = \{f_1, f_2, f_3, f_4, f_5, \ldots\ldots f_n\}\epsilon R$
$Output: O(S_C) = [0,1]$
$initialize\ n < \sqrt{a+b+\alpha}\ ; n \rightarrow no.\ of\ neurons, a, b$
$\rightarrow input, output\ neurons, \alpha\ (threshold\ [0-10]$
$begin$
  $compute\ O(L_{3,j}) = \overline{F_S}(p,q) = \frac{F_{S1}(p,q)}{F_{S1}(p,q)+F_{S2}(p,q)}$
    $compute\ O(Y) = \sum n_{fp}\ \overline{F_S}(p,q)$
    $compute\ \hat{e} = O(T) - O(Y)$
    $update\ w_e = w_{old(k)} * \beta + w_{old(k+1)}$
  $choose\ \delta = \frac{1}{2}\ln(1-\hat{e}/\hat{e})$
$update\ O(S_C) = P_{t+1} = \frac{P_{t+1}^{\overline{F_S}(p,q)\delta}}{N}$
    $update\ a, b = min\|O_{sc}\|\epsilon[-1,1]$
end

5 Results and discussion

A metaheuristic and optimized soft computing framework has been proposed and implemented in this research paper for segmentation of retinal fundus images for early detection of diabetic retinopathy and glaucoma. The fundus images have been taken from the well-known DRIVE data set as well as STARE data set, and the efficiency of the proposed method has been justified in terms of essential metrics such as sensitivity, specificity, overall accuracy, computation time and classification rate. The experimentations have been done on MATLAB software run on a Intel I5 processor with 8 GB RAM capacity running at 2.6 GHz. The different data sets have been chosen due to the varying retinal image sizes of 540 pixels diameter in case of DRIVE, while 650 pixels in case of STARE data sets. The fundus images have been preprocessed using a 3×3 mask using a hybrid mean–median filter integrated with adaptive histogram equalization obtaining the preprocessed image free of any additive and multiplicative speckle noises. The intensity peaks are also eliminated in the due process. Figure 7 depicts the original as well as preprocessed images.

The images with enhanced vessel structures which are to be segmented are given as input to the ACO algorithm for optimal feature extraction following which the vessels are classified as normal or abnormal vessels which define the objective of this research work. The efficiency of the proposed work is defined by a list of attributes, namely sensitivity, specificity, positive classification rate (PCR), negative classification rate (NPR) and the total accuracy. The measures have been computed for both DRIVE and STARE databases. The formulation of these metrics are done with the help of preliminaries such as true positive (TP), true negative (TN), false positive (FP) and false negative (FN).

Sensitivity is defined as

$$S_{es} = \frac{\text{True Positive}}{\text{True Positive} + \text{False negative}} \tag{6}$$

Specificity is defined as

$$S_{\text{ep}} = \frac{\text{True negative}}{\text{True negative} + \text{False positive}} \tag{7}$$

Overall accuracy is defined as

$$\text{Acc}(\%) = \frac{\text{True Positive} + \text{True negative}}{\text{True Positive} + \text{True negative} + \text{False positive} + \text{False negative}} \tag{8}$$

Based on the above formulated parameters, exhaustive experimentations and computations have been done which are comprehensively shown in Table 1. Table 1 lists the

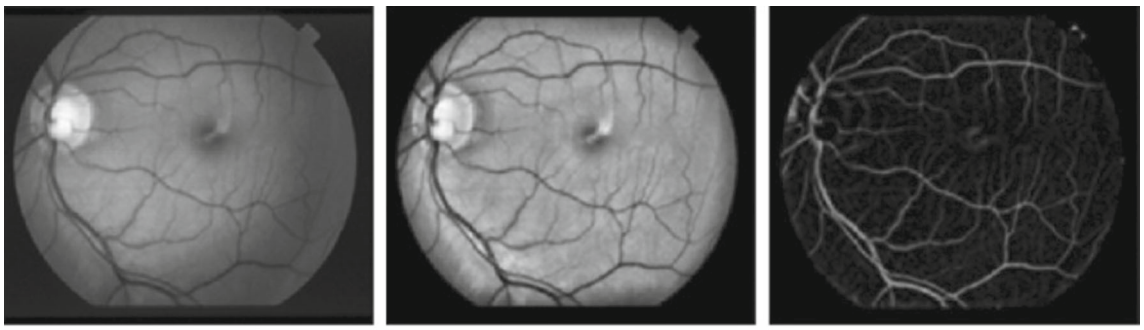

Fig. 7 **a** Gray scale image, **b** morphologically enhanced image, **c** preprocessed image (enhanced vessels)

Table 1 Sensitivity analysis of the proposed method for DRIVE and STARE

Database/sample no.	DRIVE			STARE		
	BSM	ANN	HONC	BSM	ANN	BSM
1	0.6428	0.6522	**0.7014**	0.5948	0.6158	0.6458
2	0.6154	0.6254	0.6955	0.6155	0.6356	0.7014
3	0.6954	0.7100	0.7198	0.6244	0.6954	**0.7655**
4	0.7105	0.7240	0.7356	0.5777	0.6214	0.7452
5	0.7035	0.7101	**0.8411**	0.6594	0.7014	**0.7955**
6	0.7055	0.7089	**0.7955**	0.5842	0.6545	0.7152
7	0.6988	0.7025	0.7451	0.4844	0.5944	0.6584
8	0.5486	0.6541	0.7001	0.5954	0.6425	0.6999
9	0.6541	0.6652	0.7035	0.6548	0.6948	0.7415
10	0.6021	0.6144	0.6914	0.6358	0.6999	0.7048
11	0.5984	0.6477	0.6999	0.6444	0.7015	**0.7654**
12	0.5485	0.5965	0.6589	0.5495	0.6945	**0.7865**
13	0.6044	0.6548	0.7094	0.6025	0.6948	**0.7625**
14	0.6154	0.6255	0.6988	0.6802	0.7241	**0.7954**
15	0.6485	0.6589	0.7014	0.6482	0.7411	**0.7954**

Bold indicates the justification of superiority of proposed method over other techniques

sensitivity analysis of proposed method over conventional Bayesian set model (BSM) and ANN model for segmentation and classification.

Table 2 lists the specificity analysis of proposed HONC over the BSM and ANN techniques.

Tables 1 and 2 clearly indicate the superiority of proposed method in terms of specificity and sensitivity with average values clocking around 0.7894 for DRIVE and 0.8011 for STARE in terms of sensitivity while clocking 0.8015 for DRIVE and 0.8641 for STARE set images in terms of specificity analysis over BSM and ANN models. The input image, preprocessed as well as segmented retinal image from DRIVE image set sample S_8, is shown in Fig. 8.

Table 3 presents the mean running time analysis of the three algorithms for both DRIVE and STARE databases to compute the computation overhead.

Table 3 presents the analysis of proposed method over fuzzy c-means, BSM and ANN in terms of computation time for both STARE and DRIVE databases. It could be observed that a 1.49% of computation overhead is incurred on an average for HONC over FCM and BSM due to the intense training as well as optimization process but exhibits a 0.94% reduction when compared to the conventional ANN in standalone form. The overall accuracy as computed using Eqs. (6) to (8) is presented in Fig. 9 for DRIVE database.

Figure 10 depicts the overall accuracy for both DRIVE and STARE databases, and it could be observed that proposed HONC algorithm is able to record a 98.5% improvement in the segmented output. An additional function of classification of segmented blood vessels into normal and abnormal vessels based on threshold defined in the neural classifier has also been implemented and compared against increasing number of samples as shown in

Table 2 Specificity analysis of the proposed method for DRIVE and STARE

Database/sample no.	DRIVE			STARE		
	BSM	ANN	HONC	BSM	ANN	BSM
1	0.6588	0.6859	**0.7015**	0.6954	0.7048	0.7954
2	0.4599	0.5678	0.6588	0.7142	0.7654	0.8254
3	0.6589	0.6944	0.7165	0.7415	0.7954	**0.8654**
4	0.5411	0.6014	0.6925	0.7144	0.7514	0.8141
5	0.6125	0.6748	**0.7014**	0.6599	0.7014	**0.7954**
6	0.6471	0.6944	**0.7458**	0.6944	0.7654	0.8544
7	0.6588	0.6944	0.7699	0.7077	0.7874	0.8654
8	0.7014	0.7418	0.7954	0.7541	0.7965	0.8895
9	0.7101	0.7925	**0.8411**	0.7565	0.7999	0.9014
10	0.6588	0.7014	**0.7992**	0.6582	0.7145	0.7954
11	0.6947	0.7514	0.7695	0.6451	0.7954	**0.8654**
12	0.7015	0.7325	0.7956	0.6954	0.7950	**0.9014**
13	0.6954	0.7154	0.7954	0.7017	0.7845	**0.8152**
14	0.7077	0.7255	**0.8100**	0.7451	0.8120	**0.9010**
15	0.6548	0.6925	0.7578	0.7845	0.8411	**0.9094**

Bold indicates are the justification of superiority of proposed method over other techniques

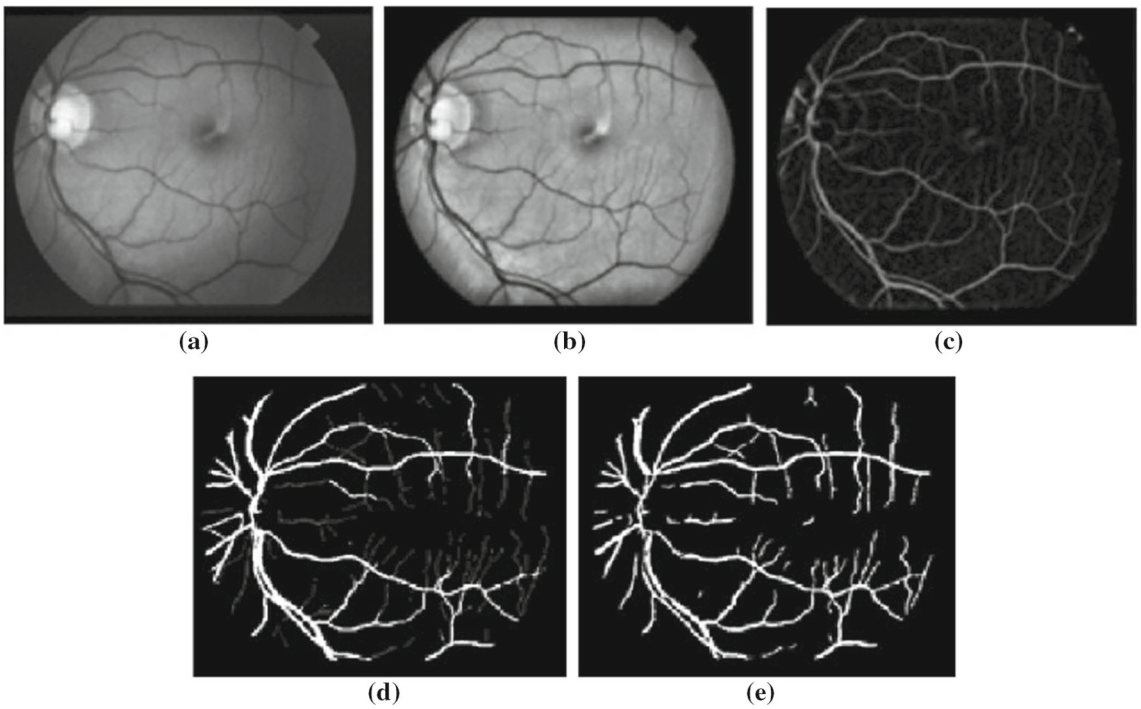

Fig. 8 **a** Input image, **b** preprocessed image, **c** vessel enhanced image, **d** vessel mapped image, **e** segmented vessel image (HONC)

Fig. 10. It could be observed that proposed HONC is able to record an average of 97.99% detection and classification accuracy which is nearly 14% more than FCM, 11.01% more than BSM and 4.32% more than ANN methods thus justifying the superiority of the proposed metaheuristic algorithm.

6 Conclusion

Retinal image classification using machine learning methods integrated with a metaheuristic approach for optimization is proposed and implemented in this research paper. The immense potential of retinal images to exhibit and provide vital statistics related to age-related disorders

Table 3 Mean running time analysis of proposed HONC for DRIVE and STARE

Database	Mean Running time (s)			
	FCM	BSM	ANN	HONC
DRIVE	10.44	12.54	13.54	13.01
STARE	11.54	14.59	16.54	15.94

like cataract formation, hypertension, diabetic retinopathy, macular disorders when systematically processed and analyzed. A machine learning technique in a hybrid combination with an optimization technique based on evolutionary process is implemented in this work. It is a two-stage processing in which the first stage generates an optimal set of feature vectors using ant colony optimization which helps to obtain optimal convergence in the least time possible with elimination of redundant data. This helps in reducing the dimension of feature vectors by about 16% accounting for 2.1% reduction in computational overhead. This optimal feature vector is subjected to a three-layer neural network model for intense learning and training for classifying the pixels into regions containing blood vessels and non-blood vessels. The accuracy of the segmentation process has been precise, and the same network is used to detect the presence/absence of abnormality in the interval [0, 1] based on a hard threshold method. Threshold values are set at 0.6 for DRIVE and 0.59 for STARE databases. Two databases have been investigated due to the varying nature of dimensions and to study the effect of them on the proposed work. Handling of high-resolution images with more optimality in terms of detection as well as classification could be researched as a future scope of this work.

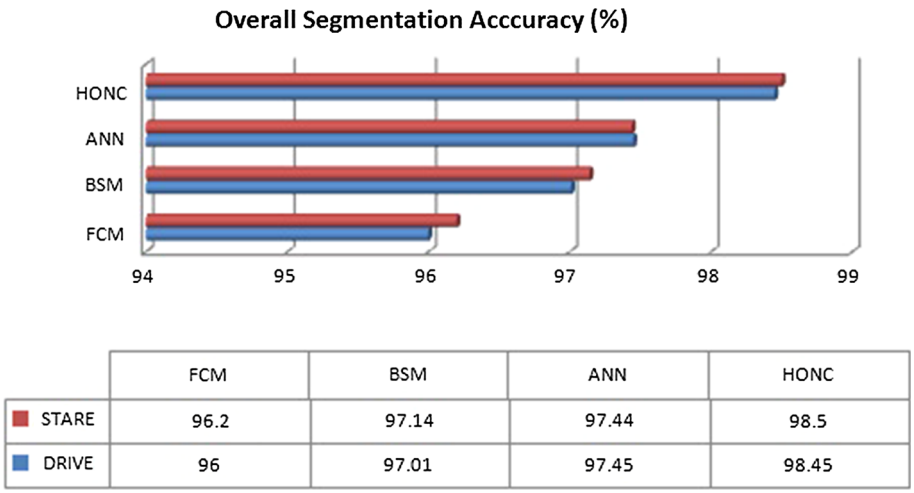

Fig. 9 Overall accuracy of segmentation using proposed HONC for DRIVE and STARE

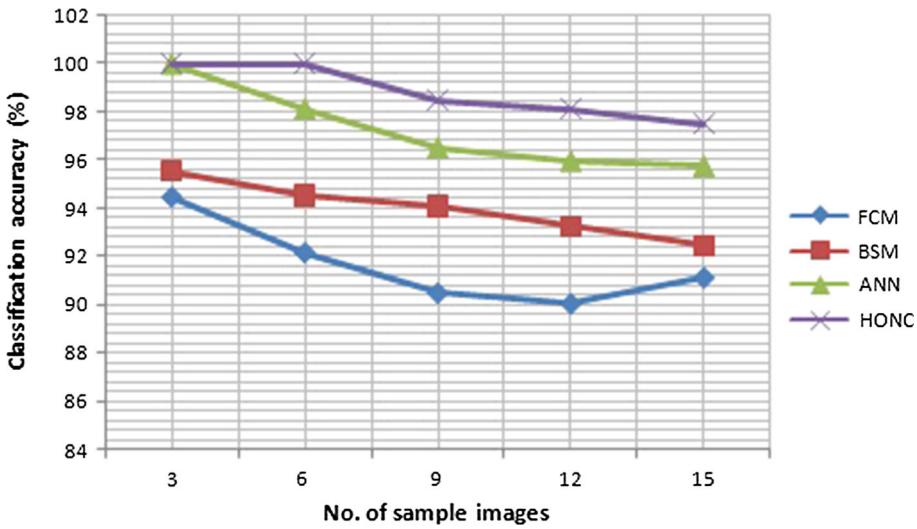

Fig. 10 Classification accuracy of the proposed HONC for normal/abnormality of blood vessels

Funding This work is not funded by any National/International bodies.

Compliance with ethical standards

Conflict of interest All authors state that there is no conflict of interest.

Human and animal rights All procedures performed in studies involving human participants were in accordance with the ethical standards of the institutional and/or national research committee and with the 1964 Helsinki declaration and its later amendments or comparable ethical standards. This article does not contain any studies with animals performed by any of the authors.

References

Das S, Biswas A, Dasgupta S, Abraham A (2009) Bacterial foraging optimization algorithm: theoretical foundations, analysis, and applications. In: Abraham A, Hassanien AE, Siarry P, Engelbrecht A (eds) Foundations of computational intelligence Volume 3. Studies in Computational Intelligence, vol 203. Springer, Berlin, pp 23–55

Elbalaoui A, Fakir M, Merbouha A (2017) Automatic detection of blood vessel in retinal images using vesselness enhancement filter and adaptive thresholding. Int J Healthc Inf Syst Inform 12:14–29

Elbalaoui A, Ouadid Y, Merbouha A (2018) Segmentation of optic disc in fundus images using an active contour. J Electron Commer Organ 16:97–111

Hoover AD, Kouznetsova V, Goldbaum M (2000) Locating blood vessels in retinal images by piecewise threshold probing of a matched filter response. IEEE Trans Med Imaging 19(3):203–210

Inoue M, Yanagawa A, Yamane S (2013) Wide-field fundus imaging using the Optos Optomap and a disposable eyelid speculum. JAMA Ophthalmolog 131:226

Kathiresan N, Samuel Manoharan J (2013) A comparative analysis of fusion based techniques based on multi resolution transforms. Natl Acad Sci Lett 38(1):61–63

Kumar R, Shimna MP (2017) Recent approaches for automatic cataract detection analysis using image processing. J Netw Commun Emerg Technol 7(10):26–31

Lee DW, Kim JM, Park KH (2010) Effect of media opacity on retinal nerve fiber layer thickness measurements by optical coherence tomography. J Ophthalmic Vis Res 5:151–157

Li Q, You J, Zhang D (2012) Vessel segmentation and width estimation in retinal images using multiscale production of matched filter responses. Expert Syst Appl 39(9):7600–7610

Lupascu CA, Tegolo D, Trucco E (2010) FABC: retinal vessel segmentation using adaboost. IEEE Trans Inf Technol Biomed 14:1267–1274

Mareli M, Twala B (2018) An adaptive cuckoo search algorithm for optimization. Appl Comput Inform 14:107–115

Marin D, Aquino A, Gegundez Aria ME, Bravo JM (2011) A new supervised method for blood vessel segmentation in retinal images by using grey level and moment invariants based features. IEEE Trans Med Imaging 30(1):146–158

Miri MS, Mahloojifar A (2011) Retinal image analysis using curvelet transform and multistructure elements morphology by reconstruction. IEEE Trans Biomed Eng 58(5):1183–1192

Nazimul H, Rohit K, Anjli H (2008) Trend of retinal diseases in developing countries. Expert Rev Opthalmol 3(1):43–50

Osareh A, Shadgar B, Markham R (2009) A computational-intelligence-based approach for detection of exudates in diabetic retinopathy images. IEEE Trans Inf Technol Biomed 13:535–545

Pereira C, Gonçalves L, Ferreira M (2015) Exudate segmentation in fundus images using an ant colony optimization approach. Inf Sci 296:14–24

Ponraj DN, Jenifer ME, Poongodi P, Samuel Manoharan J (2011) A survey on the preprocessing techniques of mammogram for the detection of breast cancer. J Emerg Trends Comput Inf Sci 2(12):656–664

Rahebi J, Hardalac F (2016) A new approach to optic disc detection in human retinal images using the firefly algorithm. Med Biol Eng Comput 54:453–461

Samuel Manoharan J (2019) A smart image processing algorithm for text recognition, information extraction and vocalization for the visually challenged. J Innov Image Process 1(1):30–38

Savastano MC, Minnella AM, Tamburrino A (2014) Differential vulnerability of retinal layers to early age-related macular degeneration: evidence by SD-OCT segmentation analysis. Invest Ophthalmol Vis Sci 55:560–566

Szénási S (2014) Distributed region growing algorithm for medical image segmentation. Int J Circuits Syst Signal Process 8(1):173–181

Vijayakumari, Suriyanarayanan N (2012) Survey on the detection methods of blood vessel in retinal images. Eur J Sci Res 68(1):83–92

Wong Y, Klein R, Sharrett AR (2002) Retinal arteriolar narrowing and risk of coronary heart disease in men and women. J Am Med Assoc 287(9):1153–1159

You X, Peng Q, Yuan Y, Cheung Y, Lei J (2011) Segmentation of retinal blood vessels using the radial projection and semi-supervised approach. Pattern Recogn 441:2314–2324